JOURNAL OF SOLID STATE CHEMISTRY 115, 229–235 (1995)

The Magnetic Properties and Structures of the Transition Metal Pyroarsenates $M_2As_2O_7$ (M = Ni, Co, Mn)

A. M. Buckley and S. T. Bramwell[1]

Inorganic Chemistry Laboratory, Oxford University, South Parks Road, Oxford OX1 3QR, United Kingdom

P. Day[2]

The Royal Institution, 21 Albemarle Street, London W1X 4BS, United Kingdom

and

D. Visser

Physics Department, Loughborough University of Technology Loughborough, United Kingdom

Received April 26, 1994; in revised form July 20, 1994; accepted July 21, 1994

The bulk magnetic properties and magnetic structures of the pyroarsenates $M_2As_2O_7$ (M = Ni, Co, Mn), whose crystal structures are related to thortveitite $Sc_2Si_2O_7$ have been investigated by susceptibility (χ) measurements and neutron powder diffraction. All three compounds behave as three-dimensional antiferromagnets. The Weiss constants θ are −92(1), −49(1), and −28(1) K, and the T_N determined from the maxima in $d\chi/dT$ are 29.1(1), 11.63(5), and 8.5(1) K, respectively. In each case, four magnetic reflections were identified in the neutron diffraction profiles below T_N. The magnetic structure of $Ni_2As_2O_7$ was refined on the basis of an approximate low-temperature crystal structure. The moments make an angle of ~30° to the c-axis in the ac-plane. Each moment has three antiparallel nearest neighbors. The antiferromagnetic sheets are further stacked in antiferromagnetic sequence along c. Comparison is made with the magnetic structure of $Mn_2P_2O_7$.

1. INTRODUCTION

Phases of composition $X_2Y_2O_7$ adopt structures belonging to two major categories, depending on whether Y is octahedrally or tetrahedrally coordinated (1). In the former, one finds pyrochlore or weberite structures but, in the latter, the structure is either that of thortveitite ($Sc_2Si_2O_7$) or one of the "dichromate" structures. In both cases where Y is tetrahedrally coordinated, anions $Y_2O_7^{n-}$ may be distinguished, either with two YO_4 sharing a vertex in a staggered conformation with Y–O–Y angle of 180° (thortveitite), or eclipsed with a smaller angle (dichromate). Several transition metal pyrophosphates and pyroarsenates (X = Ni, Co, Cu; Y = P, As) adopt the thortveitite structure at high temperature but, on cooling, undergo a transition to a structure in which the Y–O–Y unit is bent. In an earlier paper (2), we refined the high-temperature thortveitite structures of $X_2As_2O_7$ (X = Mn, Co, Ni) and found that the low-temperature structures, while closely related to thortveitite, were most probably triclinic and could not be refined from our powder data. Subsequently, it was shown that in the thortveitite structure of $Mn_2As_2O_7$ the bridging O are disordered by bending of the As–O–As (3). In this paper, we report bulk magnetic susceptibility data for the same three phases together with low-temperature neutron powder diffraction data which yield information on the ordered magnetic structures. The structure is an interesting one from a magnetic point of view because the X ions form distorted hexagonal honeycomb sheets in the ab-plane, the sheets being separated in the c-direction by the As_2O_7 units. In fact, however, the magnetic behavior is not that of a two-dimensional lattice.

2. EXPERIMENTAL AND RESULTS

2.1. Magnetic Susceptibility

The magnetic susceptibilities of samples of $M_2As_2O_7$ (M = Co, Mn, Ni), prepared as described in Ref. (2), were measured by a PAR Model 150 vibrating sample magnetometer at the Gorlaeus Laboratory, University of Leiden, between temperatures of 0 and 100 K and in a magnetic field of ~0.47 T. The temperature dependence

[1] *Present address: Institut Laue-Langevin, 156X, 38042 Grenoble Cedex, France.*

[2] To whom correspondence should be addressed.

0022-4596/95 $6.00

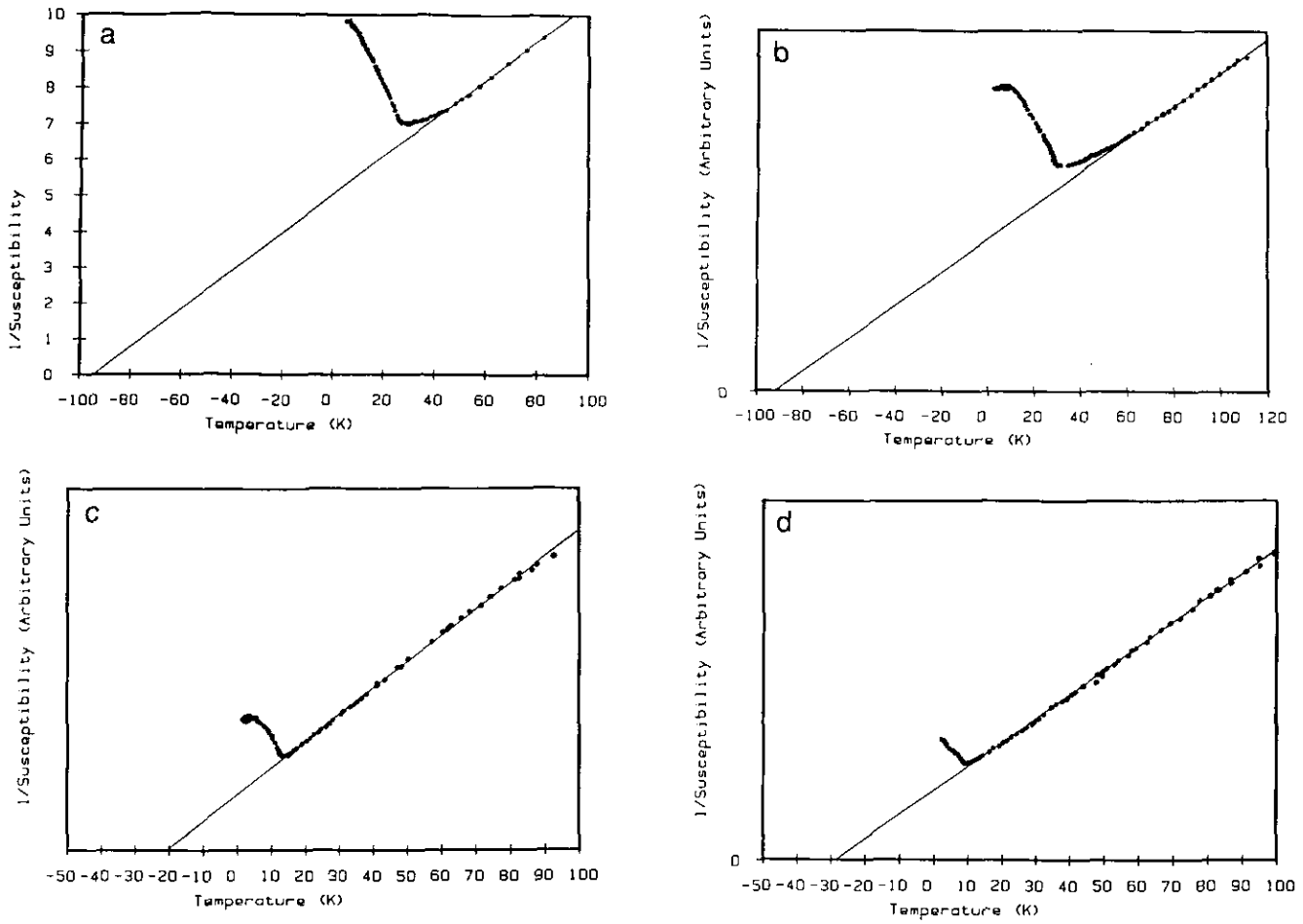

FIG. 1. Inverse susceptibility vs temperature for $M_2As_2O_7$: (a) M = Ni (Faraday Balance data), (b) M = Ni, (c) M = Co, and (d) M = Mn (b to d are VSM data).

of the inverse susceptibilities is shown in Fig. 1. Its form is characteristic of three-dimensional magnetic lattices. In the case of $Co_2As_2O_7$ and $Mn_2As_2O_7$, the Weiss constants (θ) were estimated from susceptibility data extending up to about $10T_N$ but, for $Ni_2As_2O_7$, the estimate is based on data only up to about $4T_N$. Estimates of T_N were obtained from $d\chi/dt$ versus temperature plots.

The magnetic parameters for $M_2As_2O_7$ are given in Table 1. The quantity Jz/k is estimated from the relation $q = (2/3)zS(S + 1)(J/k)$ derived from the asymptotic behavior of the high-temperature series expansion formula (4) at high T. The value to be used for the coordination number z of the magnetic lattice is not completely self-evident. The honeycomb network in the [001] plane contains three M^{2+} neighbors for each M^{2+} at distances of 3.309(7) (Mn), 3.211(7) (Co), and 3.169(2) Å (Ni), but there are two additional M^{2+} neighbors in adjacent layers at distances of 4.8025(2) (Mn), 4.7633(1) (Co), and 4.7437(1) Å (Ni). The values of J/k given in Table 1 are therefore calculated on the basis of $z = 5$.

2.2. *Zero-Field Sublattice Magnetization*

Zero-field sublattice magnetization was measured on powdered samples of α-$Co_2As_2O_7$ and α-$Ni_2As_2O_7$, using the D1B diffractometer, ILL (Grenoble), by observing the variation in intensity with temperature of the most intense magnetic reflections in the neutron diffraction profiles, measured between $2\theta = 5°$ and 90° ($\lambda = 2.52$ Å). Data were recorded at 0.5 K intervals between 2.9 and 33 K for α-$Ni_2As_2O_7$ and 2.5 to 16.5 K for α-$Co_2As_2O_7$.

The profiles of the -1, $-1\frac{1}{2}/-1\,1\frac{1}{2}$ magnetic reflections were fitted to a Gaussian function using the ILL program PKFIT (5) after subtraction of a linear baseline. Since the reflection overlaps with two nuclear reflections in the Ni compound and one in the Co, this region was fitted to three and two Gaussians, respectively. Figure 2 shows the normalized intensity (I/I_{max}) versus temperature. If I is the intensity of the magnetic Bragg reflection as the ordering temperature T_N is approached from below, and β is the critical exponent, $\log I = \log B + 2\beta \log[1 -$

TABLE 1
Magnetic Parameters for $M_2As_2O_7$ (M = Co, Mn, Ni)

	$Ni_2As_2O_7$	$Co_2As_2O_7$	$Mn_2As_2O_7$	$Mn_2P_2O_7$[a]
T_N (susceptibility) (K)	29.1(1)	11.63(5)	8.5(1)	14.0(3)
T_N (magnetization) (K)	29.3(7)	15.3(2)		
β	0.20(5)	0.20(5)		
T (χ_{max}) (K)	32.3(5)	13.67(2)	9.3(1)	
θ (K)	−92(1)	−49(1)	−28(1)	−13(1)
zJ/k (K)	−68.9(5)	−19.6(5)	−4.9(5)	−2.2(2)
J/k (z = 5) (K)	−13.8(5)	−3.92(5)	−0.98(5)	−0.45(5)
T (χ_{max})/T_N	1.11(1)	1.175(4)	− 1.094(1)	
$T_N/z\|J\|S(S+1)$	0.21(8)	0.16(8)	0.20(8)	−0.72(8)

[a] See Reference (15).

T/T_N] and B is a constant. Plots of this function are shown in Fig. 3. However, values of the critical exponent β obtained from a least-squares fit to the data points in Fig. 3 are subject to substantial uncertainty as shown in Table 1. Nevertheless, the values obtained are significantly smaller than that expected for a three-dimensional lattice (0.33).

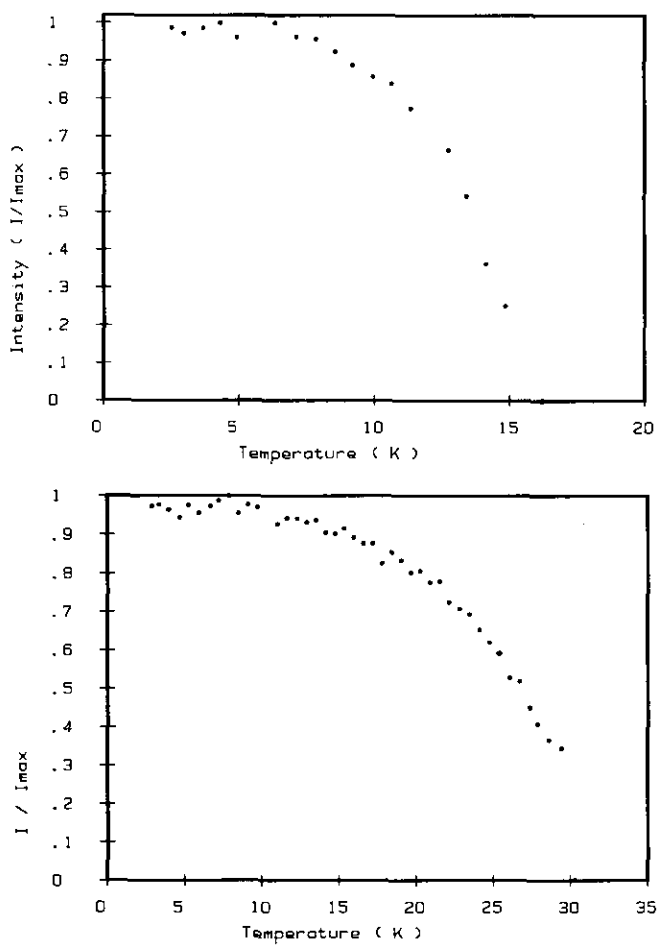

FIG. 2. (a) Zero-field sublattice magnetization of (a) $Co_2As_2O_7$ and (b) $Ni_2As_2O_7$ from intensity of the (−1 −1 1/2) magnetic reflection.

2.3. Magnetic Structures

The magnetic structures of $M_2As_2O_7$ (M = Ni, Co, and Mn) were investigated using neutron powder diffraction data obtained from the D2B and D1A diffractometers at ILL (Grenoble). Samples (about 7 g) of $M_2As_2O_7$ (M = Co, Mn, Ni) were contained in cylindrical vanadium cans in an ILL "orange" cryostat. The following diffraction profiles were obtained: (a) $Ni_2As_2O_7$ at room temperature and 5 K using D1A at a wavelength of 1.9575 Å; (b) $Co_2As_2O_7$ at room temperature and 1.5 K using D2B ("high intensity" mode) at a wavelength of 1.5963 Å; and (c) $Mn_2As_2O_7$ at 50 and 1.5 K using D2B ("high intensity" mode) at a wavelength of 1.5963 Å. No structural phase transition was observed between the higher and lower temperatures.

Comparison of the room-temperature and low-temperature neutron diffraction profiles of $M_2As_2O_7$ (M = Co, Mn, Ni) indicated at least four magnetic Bragg reflections for each compound. Each was fitted to a Gaussian function using PKFIT to obtain integrated intensities and scattering angles, which are listed in Table 2. The 2θ angles of the magnetic reflections for each compound are very similar although there are some differences in the intensity ratios.

The appearance of magnetic Bragg reflections indicates that the overall behavior of these compounds below their ordering temperatures is antiferromagnetic. Consideration of the crystallographic arrangement of magnetic ions in a sheet of $M_2As_2O_7$ (M = Co, Mn, Ni) reveals that there are 13 possible simple collinear antiferromagnetic structures (Fig. 4), depending on whether the arrangement of the magnetic sheets in the c-direction is antiferromagnetic or ferromagnetic and on the arrangement of spins within the sheet. These structures preclude doubling of the a_0- or b_0-axes only, hence possible magnetic unit cells must either be coincident with the crystallographic unit

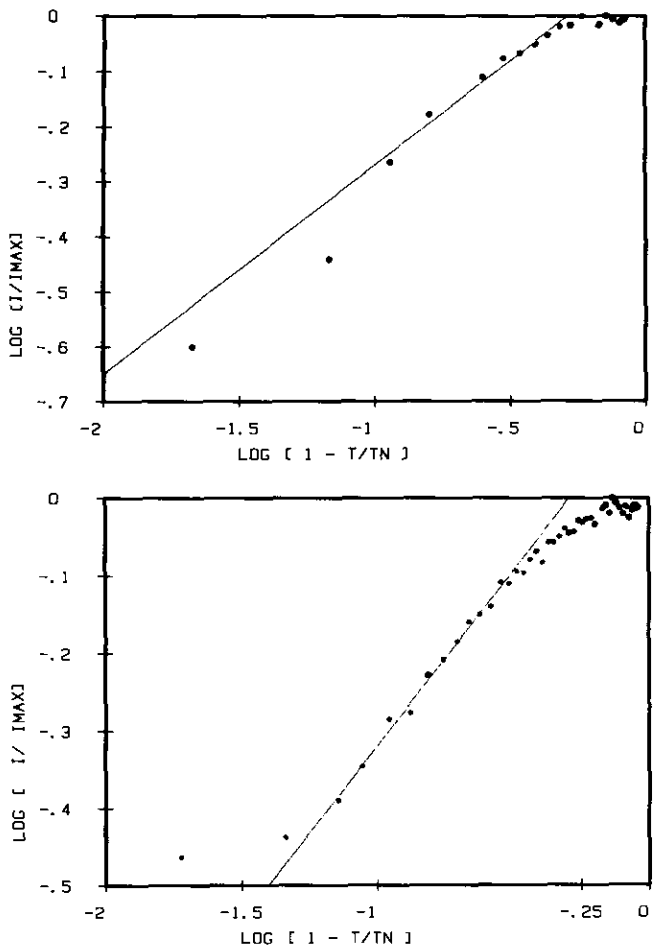

FIG. 3. Reduced plot of intensity vs temperature for (−1 −1 1/2) magnetic reflection of (a) $Co_2As_2O_7$: T_N = 15.1 K; (b) $Ni_2As_2O_7$: T_N = 30 K.

cell, be doubled in the c-direction, or be doubled in the a-, b-, and c-directions. All the observed magnetic reflections for these three compounds can be indexed on a doubled c_0-axis unit cell (Table 2) or a doubled a_0, b_0, and c_0 axis unit cell but not on the same unit cell as the crystallographic unit cell or a unit cell with a doubled a_0- and b_0-axis only. This indicates that the magnetic structures are not the same as that of $Mn_2P_2O_7$.

α-$Ni_2As_2O_7$. Since the crystal structure of α-$Ni_2As_2O_7$ is closely related to that of β-$Ni_2As_2O_7$, its high temperature (700 K) analogue, the coarse features of the crystal structure should enable the magnetic structure to be determined, providing the fit to the nuclear reflections is good enough in the low angle region.

Refinement was performed using the Rietveld method for a continuous wavelength source (6, 7). The background was removed by linear interpolation of at least 20 points. The structural model was that described earlier (2) for α-$Ni_2As_2O_7$ ($P1$). In the simplest antiferromagnetic spin arrangement, the magnetic unit cell is double the crystallographic unit cell in the c-direction. Hence, one new symmetry operator is required to describe the larger unit cell and the z-coordinates of the atom positions are halved.

In the space group $P1$, the nickel positions are unrelated by symmetry except by the new operator which transforms them into the doubled unit cell. Therefore, the sign of the magnetic moment on each ion must be specified in order to describe the magnetic structure in the ab-plane. Free ion form-factors were those of Freeman and Watson (8).

Initially a magnetic moment of 2 μ_B was placed in the $\mathbf{k}_x$-direction; $\mathbf{k}_x$, $\mathbf{k}_y$, and $\mathbf{k}_z$ were then refined together, and the R-factors were reduced to R_{mag} = 37%, R_n = 21%, R_p = 18%, R_{wp} = 16%, and R_E = 17%. The high R-factors reflect the limitations of the data but it is clear from Fig. 5 that the model l (Fig. 4) fits all the observed magnetic reflections with acceptable precision (χ^2 = 4.7). Other models, such as that of $Mn_2P_2O_7$ (Fig. 4, model d) and Fig. 4 model i) gave much poorer agreement (R_{mag} of 95 and 83%, respectively). The resulting magnitudes of the magnetic moment vector are: $\mathbf{k}_x$ = 1.0(1); $\mathbf{k}_y$ = 0.2(2); $\mathbf{k}_z$ = 1.83(6). The large esd on k_y compared with its value suggests that this component may be neglected. Hence, the magnitude of the magnetic moment/ion is 1.87 μ_B pointing 30° from the c_0-axis in the ac-plane, and the magnetic structure is as shown in Fig. 6.

α-$Co_2As_2O_7$ and $Mn_2As_2O_7$. The close relationship between the crystal structures of α-$Co_2As_2O_7$, α-$Ni_2As_2O_7$, and $Mn_2As_2O_7$, and the presence of reflections in their neutron powder diffraction profiles at similar scattering angles, indicate that the magnetic structures of the three compounds are closely similar. Indeed, the observed magnetic reflections for all three compounds may be indexed on the same magnetic unit cell (Table 2). Since the data on the Co and Mn compounds did not permit refinement of the magnetic moment vector, the magnetic moment obtained for α-$Ni_2As_2O_7$ was scaled up for these compounds, i.e., 2.34k_x and 4.42$\mathbf{k}_y$ for $Mn_2As_2O_7$ (magnetic moment/ion, 5 μ_B) and ±1.4$\mathbf{k}_x$ and ±2.6$\mathbf{k}_y$ for α-$Co_2As_2O_7$ (magnetic moment/ion, 3 μ_B). Only the scale factor was refined, in order to observe whether the magnetic structure of α-$Ni_2As_2O_7$ was close to that of α-$Co_2As_2O_7$ or $Mn_2As_2O_7$. The magnetic intensity was described well for $Mn_2As_2O_7$ and satisfactorily for α-$Co_2As_2O_7$. Table 2 compares the ratios of the calculated intensities using this method and the observed intensity ratios from the PKFIT procedure.

3. DISCUSSION

3.1. Exchange Constants and Néel Temperatures

If the coordination number of the magnetic ions z is

TABLE 2
Intensities and Scattering Angles (2θ) of Magnetic Reflections of $M_2As_2O_7$ (M = Co, Mn, Ni)

Compound	2θ (λ = 1.59 Å)	Index (doubled c_0-axis cell)	Intensity ratio (I/I_{max}) Observed	Calculated (see text)
α-$Ni_2As_2O_7$	18.53°	−1 −1 1/−1 1 1	1	
	21.90°	1 −1 1/1 1 1	0.32	
	23.77°	0 −2 1/0 2 1	0.28	
	32.13°	−1 −1 3	0.16	
α-$Co_2As_2O_7$	18.30°	−1 −1 1/−1 1 1	1	1
	21.22°	1 −1 1/1 1 1	0.18[a]	
	23.23°	0 −2 1/0 2 1	0.37	0.50
	31.83°	−1 −1 3	0.42	0.27
$Mn_2As_2O_7$	18.42°	1 1 −1	1	1
	20.94°	1 1 1		
	23.14°	0 2 1	0.16	0.23
	31.74°	1 1 −3	0.20	0.17

[a] Nuclear and magnetic reflections coincide.

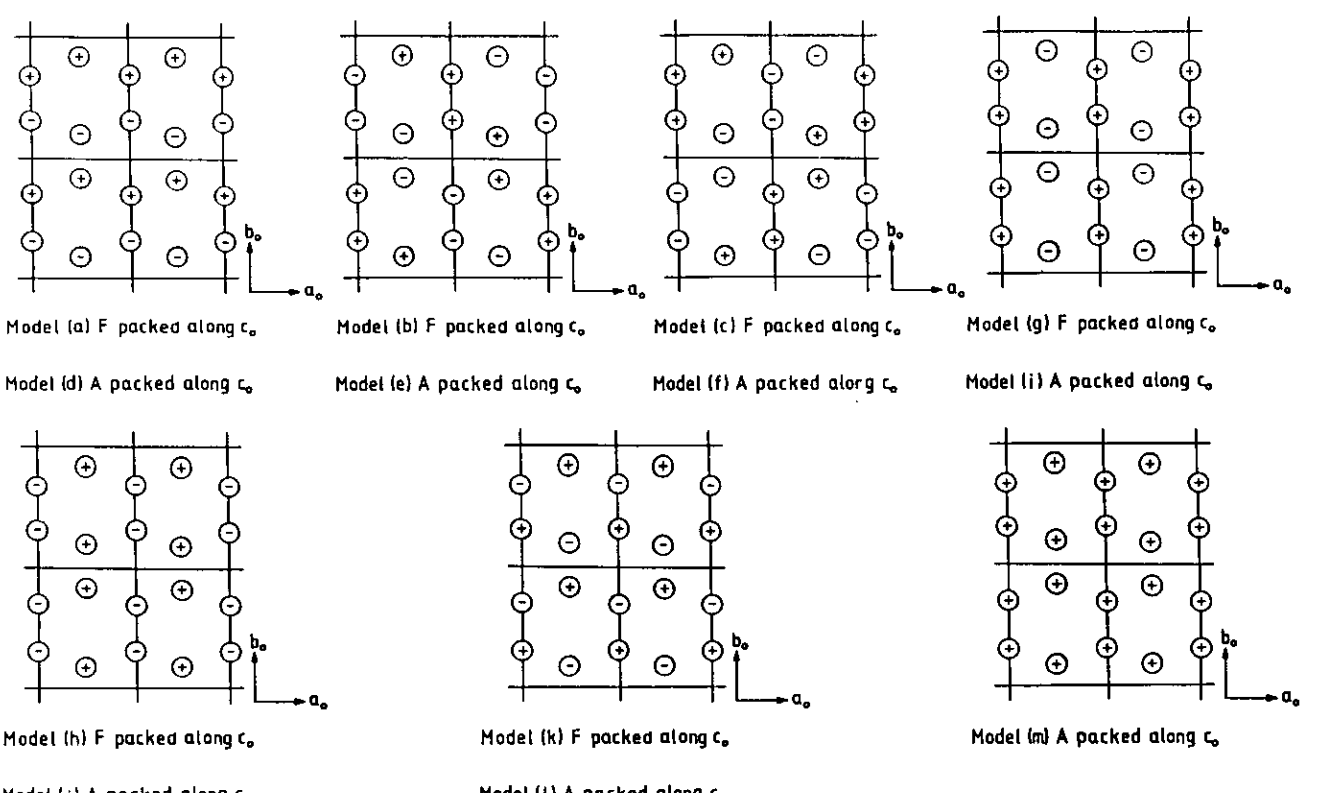

FIG. 4. The possible spin arrangements for thortveitite-type structures. F, ferromagnetic packing, and A, antiferromagnetic arrangement along Co.

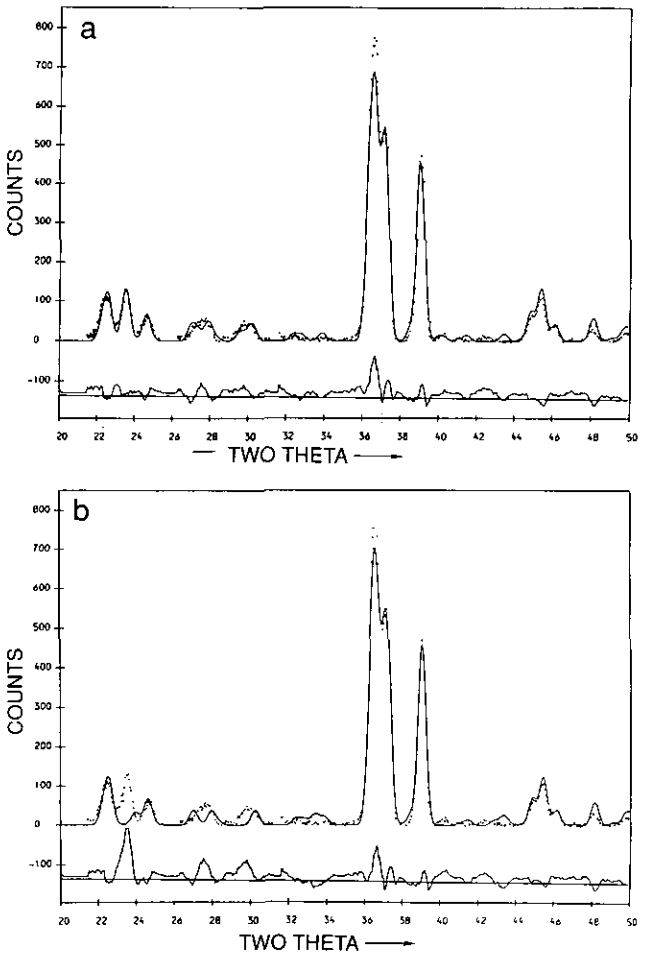

FIG. 5. Observed (dots) and calculated (full line) neutron diffraction profile α-$Ni_2As_2O_7$ with magnetic structure of Fig. 4 model I.

taken to be 5 (see Section 2.1), the exchange constants derived for $Ni_2As_2O_7$ and $Mn_2As_2O_7$ (Table 1) are of similar magnitude to those determined for other arsenates such as $KNiAsO_4$ (−11.3 K) and $MnHAsO_4 \cdot H_2O$ (−1.2 K) (9). Furthermore, the magnitude of the quantity $T_N/z|J|S(S+1)$ is the same in all the arsenate compounds, signifying comparable exchange pathways between magnetic ions. The values of $T(\chi_{max})/T_N$ are all close to those derived by Sykes and Fisher (10) for the three-dimensional Ising model, indicating three-dimensional magnetic behavior, as expected from the three-dimensional crystal structure.

$Mn_2As_2O_7$ has the weakest effective exchange interaction of the series with a correspondingly low ordering temperature T_N. The exchange interaction is directly proportional to the orbital overlap integral squared, which in turn depends upon the occupancy of the d-orbitals and how they interact with those of the intervening ligand (11). Anderson (12) has shown that for a 90° superexchange mechanism, $J(d^5)$ is expected to be much less than $J(d^8)$. In Mn^{2+} the interaction between the singly occupied e_g and t_{2g} orbitals gives rise to antiferromagnetic interactions, whereas in Ni^{2+} only the e_g orbitals are singly occupied and a ferromagnetic interaction is expected. Hence $J(d^5) \ll J(d^8)$ and T_N for $Mn_2As_2O_7$ is expected to be somewhat less than that of $Ni_2As_2O_7$. There are no direct measurements of the nearest neighbor exchange for these compounds, although the overall exchange interaction is antiferromagnetic. Experiments by other workers have shown that it is not always possible to predict the nearest neighbor exchange on the basis of the above rule (e.g., Regnault (13) for $BaM_2(AsO_4)_2$ (M = Ni, Co)), because of next-neighbor interactions. Furthermore, the M–O–M angles (2) are somewhat greater than 90° (between 100° and 107°), and this will also have some effect, since a 180° exchange interaction is expected to be antiferromagnetic.

There is little difference between the value of T_N for $Ni_2As_2O_7$ determined from the magnetization and VSM susceptibility measurements, in contrast to the values of T_N for $Co_2As_2O_7$, which are rather different. An explanation for this could be the different methods used to obtain these values. Neutron diffraction probes the order on one sublattice, and so would be sensitive to short-range order on one or two sublattices. Susceptibility is a bulk measurement and, therefore, sensitive to long-range order. It is interesting to note that T_N for $Mn_2P_2O_7$ (14.0(3) K) is somewhat greater than that for $Mn_2As_2O_7$ although the two compounds are isomorphous. Furthermore, the exchange constants for the two compounds and hence the value of $T_N/z|J|S(S+1)$ also differ. However, the latter may be a reflection of the fact that θ for the pyrophosphate was determined using higher temperature data (150–300 K) than the pyroarsenate.

The values of the critical exponents β of $Co_2As_2O_7$ and $Ni_2As_2O_7$ (Table 1) are lower than those predicted for three-dimensional magnetic behavior, i.e., $\beta = 0.312$ for

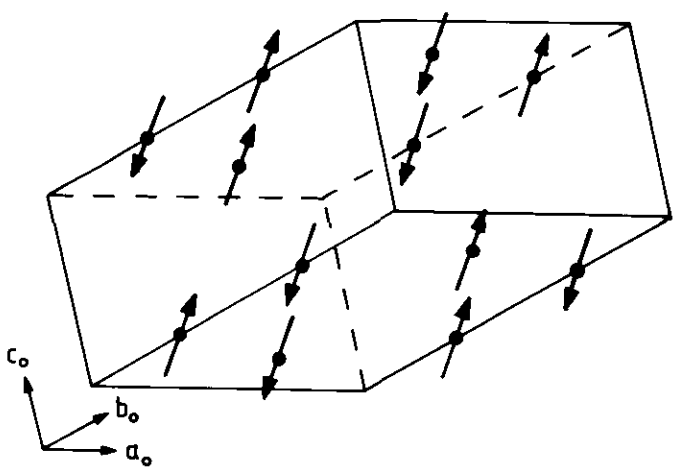

FIG. 6. Magnetic structure of α-$Ni_2As_2O_7$.

a three-dimensional Ising lattice and $\beta = 0.36$ for a three-dimensional Heisenberg lattice (14). Lower values of β may be associated with low-dimensionality (16) or frustration (17), but there is no evidence for these effects in the present compounds. It should further be pointed out that the neutron diffraction data relate to a range of temperatures extending beyond that normally considered to be the critical region.

3.2. *Magnetic Structures*

Because the crystal structure of α-$Ni_2As_2O_7$ is so closely related to that of the high temperature β-phase, it was possible to refine its magnetic structure because of the good fit of the approximate nuclear model in the low angle region of the neutron powder diffraction profile. That magnetic reflections occur in all three compounds at almost identical scattering angles indicates that the magnetic structures are similar. However, differences in the observed intensity ratios suggest that the spin direction may be different in α-$Co_2As_2O_7$ and $Mn_2As_2O_7$ from that in α-$Ni_2As_2O_7$, though it is probable that the spin lies in the *ac* plane in all three compounds. The magnetic moment per ion (1.87 μ_B) is reduced from the expected value of 2 μ_B (i.e., $g\mu_B S$) for Ni^{2+}, consistent with a reduction in the moment of 0.1 $\mu_B(1/2z$ if $z = 5)$ due to antiferromagnetic zero-point spin deviations.

The only magnetic measurements hitherto performed on pyroarsenate or pyrophosphate compounds are those on $Mn_2P_2O_7$ (15, 3). The crystal structure of α-$Ni_2As_2O_7$ is closely related to that of $Mn_2P_2O_7$, which adopts the thortveitite structure. In α-$Ni_2As_2O_7$ the moments lie at an angle of 30° from the c_0-axis in the *ac*-plane. Each moment has three antiparallel nearest neighbors corresponding to three antiferromagnetic bonds, assuming near-neighbor interaction only. These produce antiferromagnetic chains that run in three directions in the *ab*-plane. The sheets are then stacked antiferromagnetically in the *c*-direction (Fig. 6). In contrast, the magnetic structure of $Mn_2P_2O_7$ consists of ferromagnetic sheets of atoms in approximately *ac*-planes with the moments in each sheet aligned antiferromagnetically to the moments in neighboring sheets. The moments make an angle of 23° to the *a*-axis in the *ac*-plane. From an examination of the crystal structures of the two compounds, it appears that the moments are not aligned in any direction of evident crystallographic significance. The factors determining the direction of spin alignment, as well as the difference between the two magnetic structures, remain to be clarified.

ACKNOWLEDGMENTS

We thank SERC for partial support, ICI for support to A. M. Buckley, and Drs. A. Hewat and J. Cockcroft for assistance with the neutron scattering experiments.

REFERENCES

1. I. D. Brown and C. Calvo, *J. Solid State Chem.* **1,** 173 (1970).
2. A. M. Buckley, S. T. Bramwell, and P. Day, *J. Solid State Chem.* **86,** (1990).
3. M. A. G. Aranda, S. Bruque, and J. P. Attfield, *Inorg. Chem.* **30,** 2043 (1991).
4. G. S. Rushbrooke and P. J. Wood, *Mol. Phys.* **1,** 257 (1958).
5. R. S. Vaughan-Watkins, "Modification of Harwell PKFIT Program." University of Westminster, London.
6. H. M. Rietveld, *J. Appl. Crystallogr.* **2,** 65 (1969).
7. A. W. Hewat, "Harwell Report," AERE-R7350, 1973.
8. A. J. Freeman and R. E. Watson, *Acta Crystallogr.* **14,** 231 (1961).
9. S. T. Bramwell, A. M. Buckley, D. Visser, and P. Day, *Phys. Chem. Miner.* **15,** 465 (1988).
10. M. F. Sykes and M. E. Fisher, *Physica* **28,** 919 (1962).
11. J. Kanamori, *J. Phys. Chem. Solids* **10,** 87 (1959).
12. P. W. Anderson, *Solid State Phys.* **14,** 99 (1963).
13. L. P. Regnault, *et al.*, *J. Magn. Magn. Mater.* **15,** 1021 (1980).
14. H. E. Stanley, "Introduction to Phase Transitions and Critical Phenomena." Oxford Univ. Press, London/New York, 1971.
15. D. C. Fowlis and C. V. Stager, *Can. J. Phys.* **47,** 371 (1969).
16. S. T. Bramwell, and P. C. Holdsworth, *J. Phys. Condens. Matter* **5,** L53 (1993).
17. H. Kawamura, *J. Phys. Soc. Jpn.* **58,** 584 (1989).
18. M. F. Collins, G. S. Gill, and C. V. Stager, *Can. J. Phys.* **49,** 979 (1971).